SAKARYA ÜNİVERSİTESİ
FEN BİLİMLERİ ENSTİTÜSÜ DERGİSİ

Sakarya University Journal of Science
SAUJS

ISSN 1301-4048 | e-ISSN 2147-835X | Period Bimonthly | Founded: 1997 | Publisher Sakarya University | http://www.saujs.sakarya.edu.tr/

Title: Mechanism of Tunable Band Gap of Halide Cubic Perovskite CsPbBr3−xIx

Authors: Veysel ÇELİK

Recieved: 26.03.2023

Accepted: 31.08.2023

Article Type: Research Article

Volume: 27
Issue: 6
Month: December
Year: 2023
Pages: 1276-1285

How to cite
Veysel ÇELİK; (2023), Mechanism of Tunable Band Gap of Halide Cubic Perovskite CsPbBr3−xIx. Sakarya University Journal of Science, 27(6), 1276-1285, DOI: 10.16984/saufenbilder.1270814
Access link
https://dergipark.org.tr/en/pub/saufenbilder/issue/80994/1270814

Sakarya University Journal of Science 27(6), 1276-1285, 2023

Mechanism of Tunable Band Gap of Halide Cubic Perovskite $CsPbBr_{3-x}I_x$

Veysel ÇELİK *[1]

Abstract

Perovskites are organic-inorganic compounds with a crystal structure that revolutionize many optoelectronic applications, especially solar cells. The $CsPbBr_{3-x}I_x$, a perovskite, has garnered significant attention due to its tunable band gap and excellent photovoltaic properties. In this theoretical study, the structural, electronic, and optical properties of $CsPbBr_{3-x}I_x$ are investigated through density functional theory calculations. The calculations reveal that the substitution of Br with I leads to a significant reduction in the band gap of $CsPbBr_{3-x}I_x$, resulting in improved light absorption properties. The obtained data show that the coexistence of Br and I ions in the structure creates an energy level similar to the shallow energy levels caused by doping at the R symmetry point in the band structure.

Keywords: Tunable band gap, perovskite, solar cells, $CsPbBr_{3-x}I_x$, DFT

1. INTRODUCTION

In comparison to other standard photovoltaic materials, hybrid organic-inorganic perovskite photovoltaic semiconductors have attracted a considerable deal of interest in recent years and have made remarkable developments.[1-5] The power conversion efficiency (PCE) has reached a verified record of 25.7%[6] Due to its exceptional photoelectric properties, such as long carrier diffusion lengths, low trap-state densities, and large absorption coefficients.[3, 7, 8] Perovskites, with their high power conversion efficiencies and cost-effectiveness, are promising materials for solar cells. However, there are a number of technical challenges faced during the commercialization process. One of the ways to improve the performance of perovskites is by doping with cations of appropriate size. In a previous study, it was reported that doping with trace amounts of Nd^{+3} prevented ion migration.[9] The control of defects and rapid discovery of new materials is crucial for enhancing the performance of perovskite-based devices.[10] The design, characterization and evaluation of new dopant-free hole selective materials to improve the performance and stability of perovskite solar cells is one of the important research topics in this regard.[11] The use of these strategies can make the commercialization of perovskite solar cells a closer target.

The general chemical formula of perovskites is ABX_3, where X typically represents an anion like a halide (e.g., Iodine, Bromine, or Chlorine). In hybrid organic-inorganic perovskites, there is an organic molecule at

* Corresponding author: vcelik@siirt.edu.tr (V. ÇELİK)
[1] Siirt University, Türkiye
ORCID: https://orcid.org/0000-0001-5020-8422

the A site. Due to their electronic properties, $CH_3(NH_2)_2^+$ (FA) or $CH_3NH_3^+$ (MA) cation molecules are generally used in site A. Unfortunately, the presence of organic components renders perovskite compounds thermally unstable. When the temperature reaches 85 degrees Celsius, the $MAPbI_3$ film begins to disintegrate into PbI_2 and other byproducts,[12, 13] which severely restricts the production, storage, and use of the constructed devices.[14-17]

Therefore, there is an immediate need to investigate semiconductor photovoltaic materials with strong heat stability for industrial device fabrication. Completely inorganic perovskites, such as $CsPbX_3$ where X represents halide ions (e.g., Iodine, Bromine, or Chlorine), are crucial for addressing this issue In the $CsPbX_3$ structure, a Cs ion with a large ionic diameter is used instead of organic molecules such as MA and FA.[18, 19] Compared to organic-inorganic perovskite films, $CsPbI_3$ significantly improves heat resistance by delaying the onset of thermal degradation until 450°C. Moreover, the completely inorganic $CsPbX_3$ exhibits extraordinary photoelectric capabilities with high photoluminescence (PL) quantum yields, long carrier diffusion lengths, and high defect tolerance, which ensures their exceptional optoelectronic properties.[20, 21] Due to the thermal stability problems of organic-inorganic perovskites with high PCE, $CsPbI_3$, which has been examined in studies to find an alternative structure, is a very promising candidate for relatively high PCE when compared to $CsPbBr_3$ and $CsPbCl_3$ structures.[22] The band gap of the cubic phase inorganic perovskite $CsPbI_3$ is 1.73 eV, which is suitable for photovoltaic applications.[23, 24] However, the phase stability of $CsPbI_3$ is low due to the smaller radius of the Cs ion compared to organic molecules such as MA.[25] For example, the cubic phase of $CsPbI_3$ is unstable at room temperature.[22] One of the ways to overcome this problem may be to replace the I ion with the Br ion in certain ratios in the structure. Therefore, the mixed halide $CsPbBr_{3-x}I_x$ has been the subject of research.[26, 27] With the $CsPbI_2Br$ perovskite produced by appropriate engineering methods, an efficiency of over 17% was obtained.[28]

Besides stability, the band gap can be tuned by using the ratio of Br and I ions in the $CsPbBr_{3-x}I_x$ structure.[22] Studies on $CsPbBr_{3-x}I_x$ in the literature have focused on the band gap value of this material and, accordingly, the changes in its optical properties.[29-31] In addition to these studies, it would be useful to examine in more detail how the ratios of Br and I ions cause a change in the band structure to explain the electronic behavior of the material in technological applications. The obtained data will shed light on the mechanism of the proportional change of the band gap. This work aims to fill this gap and, therefore, will help us better understand the role of $CsPbBr_{3-x}I_x$ in optoelectronic applications.

In this study, a theoretical investigation of the electronic structural and optical properties of $CsPbBr_{3-x}I_x$ using density functional theory (DFT) calculations is presented. The results provide insight into the band gap tuning mechanism of $CsPbBr_{3-x}I_x$ and highlight the impact of halide composition on its electronic and optical properties. This study offers valuable insights into the design and optimization of $CsPbBr_{3-x}I_x$ based optoelectronic devices.

2. COMPUTATIONAL METHOD

Calculations in this study are based on density functional theory (DFT). DFT calculations were made using the CASTEP code based on the plane wave pseudopotential method.[32] The van der Waals density functional (vdW-DF) method was used to treat the non-covalent interactions in the system.[33, 34] The exchange-correlation energy functional is defined by the Perdew-Burke-Ernzerhof (PBE) approach.[35] The interaction between the valence electron and the ion nucleus was

described by ultra-soft pseudopotentials. The atomic configurations in the pseudopotentials used are $5s^2 5p^6 6s^1$ for Cs, $5s^2 5p^6 5d^{10} 6s^2 6p^2$ for Pb, and $4s^2 4p^5$ for Br and $4s^2 4p^5$ for I. The initial structures used in the calculations are in cubic phase. The structures created are shown in Fig. 1. The Brillouin region was sampled in all unit cells with 6x6x6 and 13x13x13 Monkhorst-Pack[36] k-point grids for geometric optimization and density of state calculations, respectively. A plane wave basis set was used to extend the wave functions up to 250 eV kinetic energy cutoff. Atomic positions and cell parameters were optimized until the forces fell below 0.05 eV/Å.

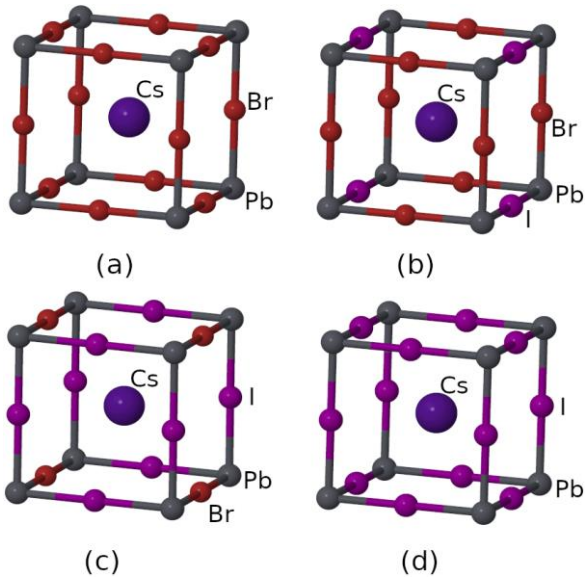

Figure 1 Optimized structures of the studied cases. (a), (b), (c) and (d) in the figure shows the optimized structures of $CsPbBr_3$, $CsPbBr_2I$, $CsPbBrI_2$ and $CsPbI_3$ cases, respectively

For qualitatively characterizing interatomic charge distributions, Bader analysis based on the atom-in-molecule (AIM) theory was employed. By integrating Bader volumes surrounding atomic sites, it is possible to determine local charge depletion/accumulation. These volumes are parts of the real space cell circumscribed by zero-flux surfaces of the charge density gradient vector field. Using a grid-based decomposition method developed by Henkelman's group,[37] the charge states of atomic species were identified in this study (Table 1).

Table 1: Bader analysis of the studied cases

	$CsPbBr_3$	$CsPbBr_2I$	$CsPbBrI_2$	$CsPbI_3$
Cs	0.84	0.90	0.85	0.84
Pb	0.68	0.69	0.61	0.44
Br	-0.51	-0.55	-0.54	-
I	-	-0.50	-0.47	-0.43

3. RESULTS AND DISCUSSION

The calculations in this study started with the $CsPbBr_3$ cubic structure. The reason for choosing the cubic structures used in the calculations is that the band gap of $CsPbI_3$ in the cubic phase has the most suitable band gap for tandem solar cells. The cubic phase is unstable at room temperature, but techniques are being developed to allow $CsPbI_3$ to retain its cubic phase for extended periods at room temperature.[18] Other structures were investigated gradually by adding the I ion instead of Br ion. Fig. 1 shows the relaxed structures without any restrictions. The structural data obtained are listed in Table 2.

The optimized structure of $CsPbBr_3$ is cubic and the length of the lattice parameters is 5.934 Å. This value is close to the values of 5.87 Å[38] and 5.85 Å[39] obtained from experimental studies. In terms of ionic radius, the I ion has larger diameter than the Br ion. Therefore, the length of the *c* lattice parameter is longer in $CsPbBr_2I$ where an I ion is found instead of a Br ion. Pb-I and Pb-Br bond lengths in the structure are 3.17 Å and 2.98 Å, respectively. Accordingly, the lengths of the lattice parameters *a*, *b* and *c* are 5.964 Å, 5.964 Å and 6.350 Å, respectively. In this process, the angle between the lattice vectors did not change and the 90 degree angle was preserved.

As a result of the increase in the number of the I ions in $CsPbBrI_2$, the length of the lattice parameter *b* increased compared to $CsPbBr_2I$. The lattice parameters *b* and *c* are equal in length and have a value of 6.346 Å. The length of the lattice parameter *a* is shorter due to the Pb-Br bond, and its value is 5.934 Å.

The angle between the lattice vectors has not changed during the optimization process, and their values have remained at 90 degrees. The optimized $CsPbI_3$ is cubic and the length of the lattice parameters is 6.319 Å. This value is close to the experimental value of 6.289 Å.[40] As can be seen in Table 2, the Cs-Br length in $CsPbBr_3$ is shorter than the Cs-I length in $CsPbI_3$. However, in in $CsPbBr_{3-x}I_x$ structures, the lengths of Cs-I and Cs-Br are isotropic, and the length of Cs-I is shorter than that of Cs-Br bonds.

Table 2 Values of structural parameters calculated for the studied cases. *a*, *b*, and *c* represent the lattice parameters. The units of length are Å

	$CsPbBr_3$	$CsPbBr_2I$	$CsPbBrI_2$	$CsPbI_3$
a	5.934	5.964	5.934	6.319
b	5.934	5.964	6.346	6.319
c	5.934	6.350	6.346	6.319
Pb-Br	2.97	2.98	2.97	-
Pb-I	-	3.17	3.17	3.16
Cs-Br	4.20	4.36	4.49	-
Cs-I	-	4.22	4.34	4.47

The results of the Bader analysis are shown in Table 1. In the cases studied, the charge sharing of the Cs atom does not change much. This is compatible with Cs energy levels below VBM and above CBM in DOS patterns. The charge loss of the Pb ion increases with the inclusion of the I ion in the system. The value of this loss is 0.44*e* in $CsPbI_3$. The charge gains of Br and I ions are close in the structures structures in which they are found together. With the increase in the I ion number in $CsPbBr_{3-x}I_x$, the electron excess of the I ion decreases. When all of the ions around Pb are I ions, the charge excess of the I ion, which has an electron excess of -0.50*e* in $CsPbBr_2I$, decreases to -0.43*e*. In connection with this, electron loss of the Pb ion decreases compared to other structures and becomes 0.44*e*.

The density of state (DOS) patterns obtained to examine the electronic structure are shown in Fig. 2. In $CsPbBr_3$, Br electrons dominate in the valence band. The edge of the valence band maximum (VBM) consists of Pb-Br hybrid energy states in which Br electrons dominate. The Cs electrons do not contribute to the VBM edge and are approximately 1.74 eV below the VBM. The Cs ion also does not contribute to the edge of the conduction band, and the empty levels of the Cs ion are about 0.24 eV above the conduction band minimum (CBM). The edge of the conduction band consists of Pb-Br empty energy levels dominated by Pb empty energy levels.

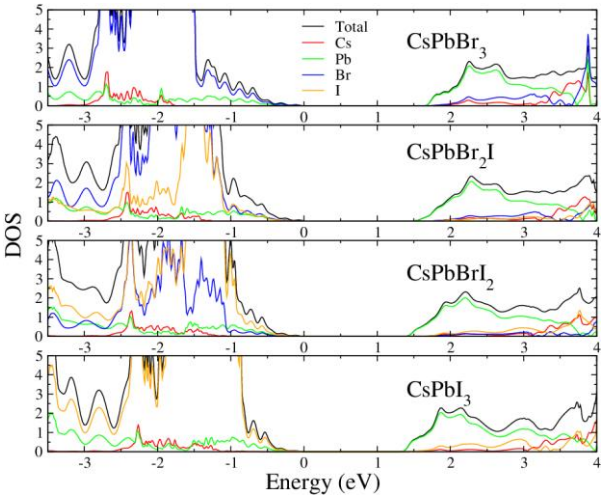

Figure 2 Obtained DOS patterns for the cases studied. Black color in graphs shows total DOS pattern. Other colors show partial DOS patterns of the ions

The characteristic of the electronic structure is semiconductor and the fermi energy level is at the top of the VBM. The value of the band gap formed between VBM and CBM is 1.68 eV. The value of the experimental band gap measured for cubic $CsPbBr_3$ is 2.23 eV.[41] The calculated value is lower than the experimental value. This error is the known error of the standard DFT, where the exchange and correlation energy cannot be fully defined. Although the calculated value in this study is lower than the experimental value, it is consistent with the values of 1.40 eV[42], 1.76 eV[43], 1.6 eV[44] calculated in previous studies. In $CsPbBr_2I$, the valence band is predominantly composed of Br-I hybrid energy levels.

The dominance of the I ion here increases in proportion to the amount of the I ion in $CsPbBrI_3$. In both structures, Cs energy levels

are located below VBM. However, in $CsPbBrI_3$, the Cs energy levels are closer to VBM. In both structures, Pb energy levels are more dominant than Br and I energy levels at the conduction band edge. The values of the band gap is 1.49 eV and 1.43 eV for $CsPbBr_2I$ and $CsPbBrI_2$, respectively. In $CsPbI_3$, the I electrons dominate in the valence band. On the conduction band side, as in the other cases, Pb empty energy levels dominate. As in the $CsPbI_3$ structure, the Cs ion does not contribute to the valence band and conduction band edges in all cases examined. The value of the calculated band gap of $CsPbI_3$ is 1.38 eV. However, this value is lower than the 1.73 eV value obtained from the previous experimental study.[45]

Fig. 3 shows the band structure of $CsPbBr_{3-x}I_x$ perovskite with different iodine concentrations. In all cases, the lowest band gap is at the R symmetry point. The transitional nature of the band gap is direct. This result is consistent with previous studies.[29, 30] The band gap decreases as the iodine content increases from 0 to 3, indicating that the addition of iodine can effectively reduce the band gap of $CsPbBr_{3-x}I_x$ perovskite. The band gap values for $CsPbBr_3$, $CsPbBr_2I$, $CsPbBrI_2$, and $CsPbI_3$ perovskite are 1.68, 1.49, 1.43, and 1.37 eV, respectively. These results indicate that with an appropriate iodine concentration, $CsPbBr_{3-x}I_x$ perovskite can have a band gap close to the optimal value for maximum solar conversion efficiency. However, it is worth noting that the thickness of the calculated structures should also be considered when making assumptions about the suitability of structures for power conversion efficiency. Fig. 4 shows the CBM band structure of the investigated cases in more detail.

In $CsPbBr_{3-x}I_x$ structures containing I and Br ions together, separate empty energy levels with close energies are formed in the CBM located at the R symmetry point. Here, lower empty energy levels are formed in proportion to the number of I ions. As a result of this decomposition, the energy difference between these energy levels in the CBM is approximately 0.18 eV in both cases. These two energy levels merge when I ions completely replace Br ions. A similar situation exists at the point of symmetry, M. The I ion pulls down the Pb empty energy levels in the CBM. There is no such separation in VBM. Fig. 5 compares the calculated VBM and CBM energy levels of the studied cases. The inclusion of I ions in certain ratios to $CsPbBr_3$ does not only narrow the band gap. It also shifts the CBM and VBM energy levels. These data are in agreement with the experimental studies on the $CsPbBr_{3-x}I_x$ structure [46].

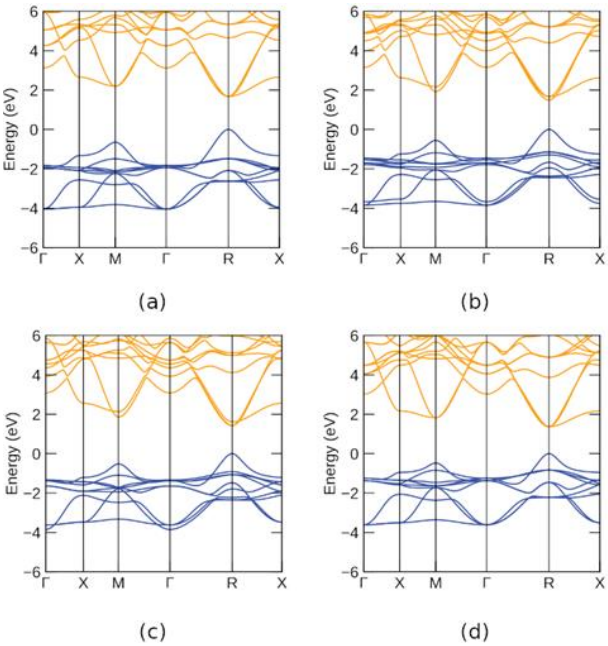

Figure 3 Obtained Band structures for the cases studied. The 0 value in the graphs represents the Fermi energy level. (a), (b), (c) and (d) in the figure shows the band structure of $CsPbBr_3$, $CsPbBr_2I$, $CsPbBrI_2$ and $CsPbI_3$ cases, respectively

In the context of perovskite solar cells, the CBM of the perovskite layer must be higher than that of the electron transport layer (ETL) to ensure efficient electron extraction and transport from the perovskite to the ETL. Accordingly, it is especially important that the CBM level can be tuned by using the ratio of the I ion in $CsPbBr_{3-x}I_x$. As the ratio of the I ions in the structure increases, the band gap

narrows and the energy levels of VBM and CBM decrease at the same time.

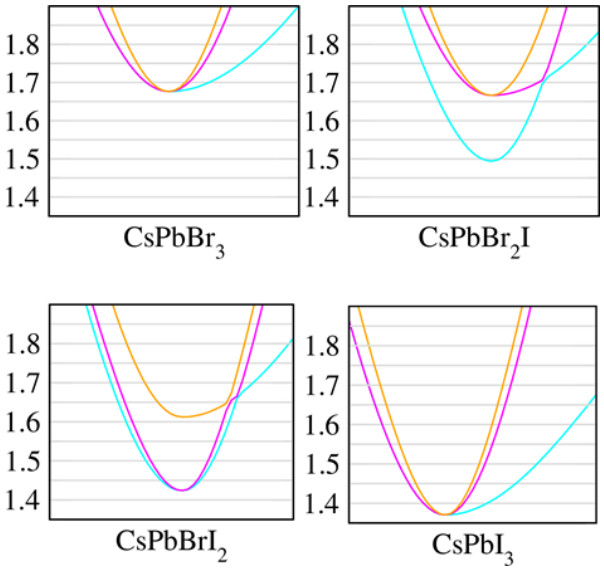

Figure 4 The more detailed view of the CBM structures. The three energy bands in the CBM are shown in different colors

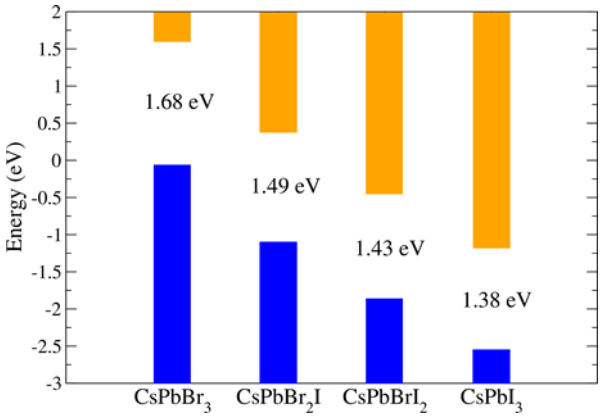

Figure 5 Comparison of VBM and CBM energy levels in electronic structures. Orange and blue colored bars represent CBM and VBM, respectively. The values between the bars indicate the value of the band gap

Fig. 6 shows the absorption coefficient plot obtained for each case. The absorption coefficient plot is compatible with the obtained DOS and band structures. As the ratio of the I ion increases in $CsPbBr_{3-x}I_x$ cases, the plot of the absorption coefficient shifts to red. This is associated with the narrowing of the band gap. The shoulder region, which has a top of 1.89 eV in the $CsPbBr_3$ pattern in the plot, begins to become obscure with the incorporation of the I ion into the structure. When compared in terms of absorption coefficient, the addition of the I ion increases the absorption coefficient of $CsPbBr_3$ in the visible region of the light spectrum.

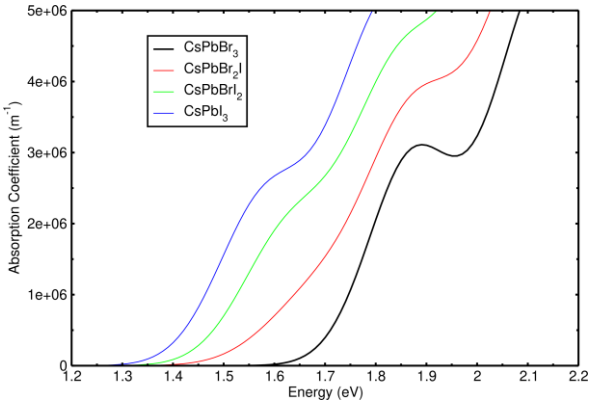

Figure 6 Obtained absorption coefficient plot for the cases

4. CONCLUSION

The study revealed that the incorporation of iodine ions into the $CsPbBr_3$ lattice can lead to a significant reduction in the band gap energy, making it a promising candidate for photovoltaic and optoelectronic applications. The data obtained in this study are especially important for the $CsPbBr_{3-x}I_x$ structure. Studies on this structure in the literature have focused on the effect of the I and Br ratios on the band gap.[29-31] In this study, the conduction band was investigated in more detail. The obtained data show that the coexistence of Br and I ions in the structure creates an energy level similar to the shallow energy levels caused by doping at the R symmetry point in the band structure. Two degenerate energy levels occur here.

The two energy levels close to each other are formed in the CBM. The lower energy of these energy levels is due to the I ion, while the higher energy is due to the Br ion. This is valid for the Br ion. Accordingly, two energy levels are formed whose state densities can be controlled using the ratio of Br and I ions. Two energy levels close together in the CBM will increase the area of the perovskite where it can harvest light. Based on this mechanism in CBM, it can be said that doping $CsPbBr_3$

with I ions at certain rates will positively affect the efficiency of the $CsPbBr_3$ perovskite. Another result obtained is that the ratio of I ions in $CsPbBr_{3-x}I_x$ changes with the value of CBM and VBM energy levels. As the ratio of I ions increases, CBM and VBM levels are drawn to lower levels. This situation can be used in perovskite-based solar cells consisting of layers. In the context of perovskite solar cells, the CBM of the perovskite layer must be higher than that of the electron transport layer (ETL)

Funding
The author has no received any financial support for the research, authorship or publication of this study.

The Declaration of Conflict of Interest/ Common Interest
No conflict of interest or common interest has been declared by the authors.

The Declaration of Ethics Committee Approval
This study does not require ethics committee permission or any special permission.

The Declaration of Research and Publication Ethics
The authors of the paper declare that they comply with the scientific, ethical and quotation rules of SAUJS in all processes of the paper and that they do not make any falsification on the data collected. In addition, they declare that Sakarya University Journal of Science and its editorial board have no responsibility for any ethical violations that may be encountered, and that this study has not been evaluated in any academic publication environment other than Sakarya University Journal of Science.

REFERENCES

[1] Y. Wang, X. Liu, T. Zhang, X. Wang, M. Kan, J. Shi, Y. Zhao, "The role of dimethylammonium iodide in cspbi3 perovskite fabrication: Additive or dopant?," Angewandte Chemie International Edition, vol. 58, no. 46, pp. 16691-16696, 2019.

[2] S. A. Veldhuis, P. P. Boix, N. Yantara, M. Li, T. C. Sum, N. Mathews, S. G. Mhaisalkar, "Perovskite materials for light-emitting diodes and lasers," Advanced Materials, vol. 28, no. 32, pp. 6804-6834, 2016.

[3] W. Xiang W. Tress, "Review on recent progress of all-inorganic metal halide perovskites and solar cells," Advanced Materials, vol. 31, no. 44, pp. 1902851, 2019.

[4] G. E. Eperon, C. E. Beck, H. J. Snaith, "Cation exchange for thin film lead iodide perovskite interconversion," Materials Horizons, vol. 3, pp. 63-71, 2016.

[5] F. Wei, Z. Deng, S. Sun, F. Xie, G. Kieslich, D. M. Evans, M. A. Carpenter, P. D. Bristowe, A. K. Cheetham, "The synthesis, structure and electronic properties of a lead-free hybrid inorganic-organic double perovskite $(MA)_2KBiCl_6$ (MA = methylammonium)," Materials Horizons, vol. 3, pp. 328-332, 2016.

[6] NREL, "National renewable energy laboratory (nrel), best research-cell efficiency chart," 2023.

[7] J. Liang, J. Liu, Z. Jin, "All-inorganic halide perovskites for optoelectronics: Progress and prospects," Solar RRL, vol. 1, no. 10, pp. 1700086, 2017.

[8] Y. Wang H. Sun, "All-inorganic metal halide perovskite nanostructures: From photophysics to light-emitting applications," Small Methods, vol. 2, no. 1, pp. 1700252, 2018.

[9] Y. Zhao, I. Yavuz, M. Wang, M. H. Weber, M. Xu, J.-H. Lee, S. Tan, T. Huang, D. Meng, R. Wang, J. Xue, S.-J.

Lee, S.-H. Bae, A. Zhang, S.-G. Choi, Y. Yin, J. Liu, T.-H. Han, Y. Shi, H. Ma, W. Yang, Q. Xing, Y. Zhou, P. Shi, S. Wang, E. Zhang, J. Bian, X. Pan, N.-G. Park, J.-W. Lee, Y. Yang, "Suppressing ion migration in metal halide perovskite via interstitial doping with a trace amount of multivalent cations," Nature Materials, vol. 21, pp. 1396-1402, Dec 2022.

[10] N. Isleyen, A. Corcor, S. Cakirefe, N. Ormanli, E. N. Kanat, I. Yavuz, "Accelerated discovery of defect tolerant organo-halide perovskites," Journal of Materials Chemistry C, vol. 10, pp. 18385-18392, 2022.

[11] J. Kruszyńska, F. Sadegh, M. J. Patel, E. Akman, P. Yadav, M. M. Tavakoli, S. K. Gupta, P. N. Gajjar, S. Akin, D. Prochowicz, "Effect of 1,3-disubstituted urea derivatives as additives on the efficiency and stability of perovskite solar cells," ACS Applied Energy Materials, vol. 5, pp. 13617-13626, 2022.

[12] B. Conings, J. Drijkoningen, N. Gauquelin, A. Babayigit, J. D'Haen, L. D'Olieslaeger, A. Ethirajan, J. Verbeeck, J. Manca, E. Mosconi, F. D. Angelis, H. G. Boyen, "Intrinsic thermal instability of methylammonium lead trihalide perovskite," Advanced Energy Materials, vol. 5, no. 15, pp. 1500477, 2015.

[13] J. K. Nam, S. U. Chai, W. Cha, Y. J. Choi, W. Kim, M. S. Jung, J. Kwon, D. Kim, J. H. Park, "Potassium incorporation for enhanced performance and stability of fully inorganic cesium lead halide perovskite solar cells," Nano Letters, vol. 17, pp. 2028-2033, Mar 2017.

[14] Z. Yao, Z. Jin, X. Zhang, Q. Wang, H. Zhang, Z. Xu, L. Ding, S. F. Liu, "Pseudohalide (SCN^-)-doped $CsPbI_3$ for high-performance solar cells," Journal of Materials Chemistry C, vol. 7, pp. 13736-13742, 2019.

[15] Q. Tai, P. You, H. Sang, Z. Liu, C. Hu, H. L. W. Chan, F. Yan, "Efficient and stable perovskite solar cells prepared in ambient air irrespective of the humidity," Nature Communications, vol. 7, p. 11105, Apr 2016.

[16] Z. Xiao, W. Meng, B. Saparov, H.-S. Duan, C. Wang, C. Feng, W. Liao, W. Ke, D. Zhao, J. Wang, D. B. Mitzi, Y. Yan, "Photovoltaic properties of two-dimensional $(CH_3NH_3)_2Pb(SCN)_2I_2$ perovskite: A combined experimental and density functional theory study," The Journal of Physical Chemistry Letters, vol. 7, pp. 1213-1218, Apr 2016.

[17] G. Niu, W. Li, F. Meng, L. Wang, H. Dong, Y. Qiu, "Study on the stability of $CH_3NH_3PbI_3$ films and the effect of post-modification by aluminum oxide in all-solid-state hybrid solar cells," Journal of Materials Chemistry A, vol. 2, pp. 705-710, 2014.

[18] T. Zhang, M. I. Dar, G. Li, F. Xu, N. Guo, M. Grätzel, Y. Zhao, "Bication lead iodide 2d perovskite component to stabilize inorganic α-$CsPbI_3$ perovskite phase for high-efficiency solar cells," Science Advances, vol. 3, no. 9, pp. e1700841, 2017.

[19] N. Li, Z. Zhu, J. Li, A. K.-Y. Jen, L. Wang, "Inorganic $CsPb_{1-x}Sn_xIBr_2$ for efficient wide-band gap perovskite solar cells," Advanced Energy Materials, vol. 8, no. 22, pp. 1800525, 2018.

[20] S. Dastidar, S. Li, S. Y. Smolin, J. B. Baxter, A. T. Fafarman, "Slow electron-hole recombination in lead iodide perovskites does not require a molecular dipole," ACS Energy Letters, vol. 2, pp. 2239-2244, Oct 2017.

[21] Q. Jing, M. Zhang, X. Huang, X. Ren, P. Wang, Z. Lu, "Surface passivation of mixed-halide perovskite $CsPb(Br_xI_{1-x})_3$ nanocrystals by selective etching for improved stability," Nanoscale, vol. 9, pp. 7391-7396, 2017.

[22] L. Protesescu, S. Yakunin, M. I. Bodnarchuk, F. Krieg, R. Caputo, C. H. Hendon, R. X. Yang, A. Walsh, M. V. Kovalenko, "Nanocrystals of Cesium Lead Halide Perovskites ($CsPbX_3$, X = Cl, Br, and I): Novel Optoelectronic Materials Showing Bright Emission with Wide Color Gamut", Nano Letters, vol. 15 (6), 3692-3696, 2015.

[23] G. E. Eperon, S. D. Stranks, C. Menelaou, M. B. Johnston, L. M. Herz, H. J. Snaith, "Formamidinium lead trihalide: a broadly tunable perovskite for efficient planar heterojunction solar cells", Energy & Environmental Science, vol. 7, pp. 982-988, 2014.

[24] K. Chen, Q. Zhong, W. Chen, B. Sang, Y. Wang, T. Yang, Y. Liu, Y. Zhang, H. Zhang, "Short-chain ligand-passivated stable $CsPbI_3$ quantum dot for all-inorganic perovskite solar cells," Advanced Functional Materials, vol. 29, no. 24, pp. 1900991, 2019.

[25] Goldschmidt, V.M., "Die Gesetze der Krystallochemie," Naturwissenschaften, 14, 477-485, 1926.

[26] S. Mariotti, O. S. Hutter, L. J. Phillips, P. J. Yates, B. Kundu, K. Durose, "Stability and performance of $CsPbI_2Br$ thin films and solar cell devices," ACS Applied Materials & Interfaces, vol. 10, pp. 3750-3760, Jan 2018.

[27] E. Akman, T. Ozturk, W. Xiang, F. Sadegh, D. Prochowicz, M. M. Tavakoli, P. Yadav, M. Yilmaz, S. Akin, "The effect of B-site doping in all-inorganic $CsPbI_xBr_{3-x}$ absorbers on the performance and stability of perovskite photovoltaics," Energy & Environmental Science., vol. 16, pp. 372-403, 2023.

[28] T. Ozturk, E. Akman, A. E. Shalan, S. Akin, "Composition engineering of operationally stable $CsPbI_2Br$ perovskite solar cells with a record efficiency over 17%," Nano Energy, Volume 87, pp. 106157, 2021.

[29] Z. Lin, J. Lei, P. Wang, X. Zhang, L. Xu, M. Chen, Y. Kang, G. Wei, "Density functional study of structural, electronic and optical properties of bromine-doped $CsPbI_3$ with the tetragonal symmetry," Journal of Alloys and Compounds, pp. 162165, vol 892, 2022.

[30] P. M. Maleka, R. S. Dima, O. M. Ntwaeaborwa, R. R. Maphanga, "Density functional theory study of Br doped $CsPbI_3$ perovskite for photovoltaic and optoelectronic applications," Physica Scripta, vol. 98, no. 4, pp. 045505, 2023.

[31] Guan Z, Wu Y, Wang P, Zhang Q, Wang Z, Zheng Z, Liu Y, Dai Y, Whangbo M-H, Huang B. "Perovskite photocatalyst $CsPbBr_{3-x}I_x$ with a bandgap funnel structure for H2 evolution under visible light," Applied Catalysis B: Environmental, vol. 245, pp. 522-527, 2019.

[32] S. J. Clark, M. D. Segall, C. J. Pickard, P. J. Hasnip, M. J. Probert, K. Refson, M. Payne, "First principles methods using CASTEP," Z. Kristall., vol. 220, pp. 567-570, 2005.

[33] E. McNellis, J. Meyer, K. Reuter, "Azobenzene at coinage metal surfaces: Role of dispersive van der Waals interactions," Physical Review B, vol. 80, pp. 205414, 2009.

[34] A. Tkatchenko M. Scheffler, "Accurate molecular van der waals interactions from ground-state electron density and free-atom reference data," Physical Review Letters, vol. 102, pp. 073005, 2009.

[35] J. P. Perdew, K. Burke, M. Ernzerhof, "Generalized gradient approximation made simple," Physical Review Letters, vol. 77, pp. 3865-3868, 1996.

[36] H. J. Monkhorst J. D. Pack, "Special points for Brillouin-zone integrations," Physical Review B, vol. 13, pp. 5188-5192, 1976.

[37] W. Tang, E. Sanville, G. Henkelman, "A grid-based bader analysis algorithm without lattice bias," Journal of Physics: Condensed Matter, vol. 21, pp. 084204, jan 2009.

[38] M. Ahmad, G. Rehman, L. Ali, M. Shafiq, R. Iqbal, R. Ahmad, T. Khan, S. Jalali-Asadabadi, M. Maqbool, I. Ahmad, "Structural, electronic and optical properties of cspbx3 (x=cl, br, i) for energy storage and hybrid solar cell applications," Journal of Alloys and Compounds, vol. 705, pp. 828–839, 2017.

[39] P. Cottingham R. L. Brutchey, "On the crystal structure of colloidally prepared cspbbr3 quantum dots," Chemical Communications, vol. 52, pp. 5246-5249, 2016.

[40] D. Trots S. Myagkota, "High-temperature structural evolution of caesium and rubidium triiodoplumbates," Journal of Physics and Chemistry of Solids, vol. 69, no. 10, pp. 2520–2526, 2008.

[41] K. Heidrich, W. Schäfer, M. Schreiber, J. Söchtig, G. Trendel, J. Treusch, T. Grandke, H. J. Stolz, "Electronic structure, photoemission spectra, and vacuum-ultraviolet optical spectra of $CsPbCl_3$ and $CsPbBr_3$," Physical Review B, vol. 24, pp. 5642-5649, Nov 1981.

[42] Y. Yang, C. Hou, T.-X. Liang, "Energetic and electronic properties of cspbbr3 surfaces: a first-principles study," Physical Chemistry Chemical Physics, vol. 23, pp. 7145-7152, 2021.

[43] H. M. Ghaithan, Z. A. Alahmed, S. M. H. Qaid, and A. S. Aldwayyan, "Structural, electronic, optical properties of $CsPb(Br_{1-x}Cl_x)_3$ perovskite: First-principles study with PBE-GGA and mbj-GGA methods," Materials, vol. 13, no. 21, 2020.

[44] Maji, P., Sadhukhan, P. Das, S. "Optoelectronic properties of facile synthesized orthorhombic cesium lead bromide ($CsPbBr_3$)," Journal of Materials Science: Materials in Electronics, 31(19), pp. 17100-17109, 2020.

[45] M. R. Filip, G. E. Eperon, H. J. Snaith, F. Giustino, "Steric engineering of metal-halide perovskites with tunable optical band gaps," Nature Communications, vol. 5, pp. 5757, Dec 2014.

[46] C. H. Ng, T. S. Ripolles, K. Hamada, S. H. Teo, H. N. Lim, J. Bisquert, S. Hayase, "Tunable open circuit voltage by engineering inorganic cesium lead bromide/iodide perovskite solar cells," Scientific Reports, vol. 8, pp. 2482, Feb 2018.